Microelectronics Journal, 25 (1994) 675–690

Review paper

III–V semiconductor waveguiding devices using adiabatic tapers

I. Moerman, G. Vermeire, M. D'Hondt, W. Vanderbauwhede, J. Blondelle, G. Coudenys, P. Van Daele and P. Demeester

Department of Information Technology — IMEC, University of Gent, Sint-Pietersnieuwstraat 41, B-9000 Gent, Belgium

In the past few years much effort has been put into the fabrication and optimization of III–V semiconductor waveguiding devices with integrated adiabatic mode size converters (tapers). By integrating a taper with a waveguide device, one wants to reduce the coupling losses and the packaging cost of OEICs in future optical communication systems. This paper gives an overview of different taper designs, their performance and the technological approaches used in realizing such tapered devices.

1. Introduction

Optical communication systems are expected to play an increasingly important role in the transmission and processing of huge amounts of data. Due to the very large bandwidth of an optical glass fibre, several optical signals can share the same fibre (wavelength division multiplexing, WDM), enabling very high transmission capacities. A typical long haul optical communication system consists of emitters, optical amplifiers, switching networks, detectors and optical fibre links. A WDM-optical network also includes wavelength multiplexers-demultiplexers and optical filters.

Not only in long haul fibre transmission systems but also in highly advanced computer networks and electronic systems is there a need for optical links. Optical interconnections allow an increase in the bandwidth and the integration density as compared to electrical interconnections.

Most optical network building blocks can be made of III–V semiconductor materials. Many high quality opto-electronic waveguiding devices, such as laser diodes, photodiodes, amplifiers, optical switches, and so on, have already been demonstrated. In the optical network, each of these devices is connected to at least one optical fibre. It is thus very important to obtain an efficient coupling of light between the fibre and the opto-electronic device. The very small refractive index difference in a glass fibre ($\Delta n < 5 \times 10^{-3}$) results in a weakly guided optical mode with a typical mode size of 8–10 μm. In semiconductor waveguiding devices, such small refractive index differences can only be achieved with extremely small compositional changes. In an optimized

0026–2692/94/$7·00

semiconductor waveguide component, Δn is generally larger than 1×10^{-2}, leading to mode sizes smaller than $2\,\mu m$. Besides, unlike the circular mode in a fibre, the mode shape in a semiconductor device is highly asymmetric, resulting in a mode mismatch between the fibre mode and the semiconductor waveguide mode. Furthermore, the optimal mode size can be different for different types of waveguide components. It is clear that the coupling loss between an opto-electronic device and a fibre is a significant part of the power budget in an optical network.

There are several approaches to improve the fibre-chip coupling efficiency, such as the use of micro-optical alignment tools (e.g. micro-lenses) or tapered/lensed fibres. However, such approaches still suffer from the field mismatch problem, since only the size and not the shape of the optical mode is converted. When using micro-lenses or tapered/lensed fibres, the reduction in coupling loss is usually at the expense of the alignment tolerance, resulting in very high packaging costs, which can be as high as 90% of the total device cost. During the past few years, many researchers have thus focused on the integration of mode size converters with opto-electronic waveguide components, in order to achieve a larger and more symmetric near field pattern at the device facet. The latter approach allows larger alignment tolerances and hence much lower packaging costs.

In the specific case of the integration of spot size converters with semiconductor lasers, there is even a twofold advantage: in addition to the improvement in coupling efficiency, there is also an increase in the operating lifetime and the maximum output power [1]. Generally, a laser with an optimized active region for a low threshold current has a wide beam (Fig. 1a). To reduce the beam divergence, one can decrease the active layer thickness, but this results in a high threshold current (Fig. 1b). When a spot-size converter is integrated with the laser, the optical mode will spread due to the thinner active layer near the laser mirror, and a narrow beam is emitted (Fig. 1c). In this way, the low threshold current, which is determined by the thicker active layer in the inner region, can be maintained. Furthermore, the large mode-size near the laser mirror enables the reduction of the optical power density, so that the catastrophic optical damage (COD) power level becomes higher, meaning that the maximum output power and operating lifetime increases.

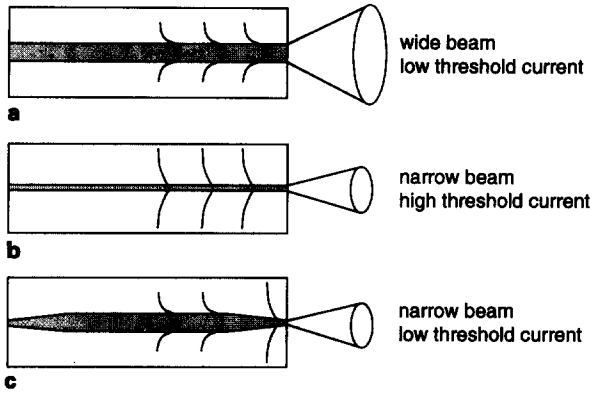

Fig. 1. Optimization of beam divergence of a laser diode by reduction of the active layer thickness.

This paper gives an overview of the different technological approaches towards the monolithic integration of mode size converters (or tapers) with III–V semiconductor waveguiding devices. In section 2 we discuss a simplified adiabaticity criterion for the design of low loss mode size converters and how to reduce the fibre-chip coupling loss. Section 3.1 gives an overview of the design of some mode size converters realized by different research groups. In section 3.2, the different technologies used to fabricate those mode size converters are described. Finally, section 4 gives an overview of the performances that have already been achieved with tapered waveguides and tapered laser diodes.

2. Adiabatic tapers

An ideal adiabatic taper for improved fibre-chip coupling transforms the small asymmetric field profile at the input of the taper into a large circular field at the end facet of the taper without any loss of power. To meet the adiabaticity condition, the taper must be carefully designed. Although it is not our intention to give rules for the design of an optimal adiabatic taper, we do provide some insight into factors which can affect taper performance. For a more general and theoretical approach, we refer to the work of Haes, Love and Black [2–4].

Suppose we have a three-layer symmetric slab waveguide of thickness d (see Fig. 2a). The refractive indices of the guiding layer and cladding layers are n_1 (resp. n_2). The width of the optical mode is dependent on the thickness of the waveguide layer and the refractive index difference $\Delta n = n_1 - n_2$. As an example, the dependence of the 1/e width of the optical mode [5] and the $(1/e)^2$ width of the beam divergence [6] are given in Fig. 3 for an InGaAsP/InP slab waveguide, guiding light at 1.55 μm. The guiding layer is InGaAsP with a bandgap wavelength of 1.3 μm and a refractive index $n_1 = 3.40$ at $\lambda = 1.55\,\mu$m, the cladding layers are InP ($n_2 = 3.18$ at $\lambda = 1.55\,\mu$m). In this example, the refractive index difference Δn is constant. To achieve a large optical mode size and thus a narrow beam divergence, one can either decrease or increase the thickness d of the guiding layer. We observe that for thin guiding layers, the width of the optical mode increases rapidly as d decreases, while for thick guiding layers, the width changes quite slowly with respect to the thickness d. We already feel intuitively that down-tapering will be much more critical than up-tapering.

The criterion for approximately adiabatic propagation, developed by J.D. Love [3] and applied on a symmetric slab waveguide, states that the

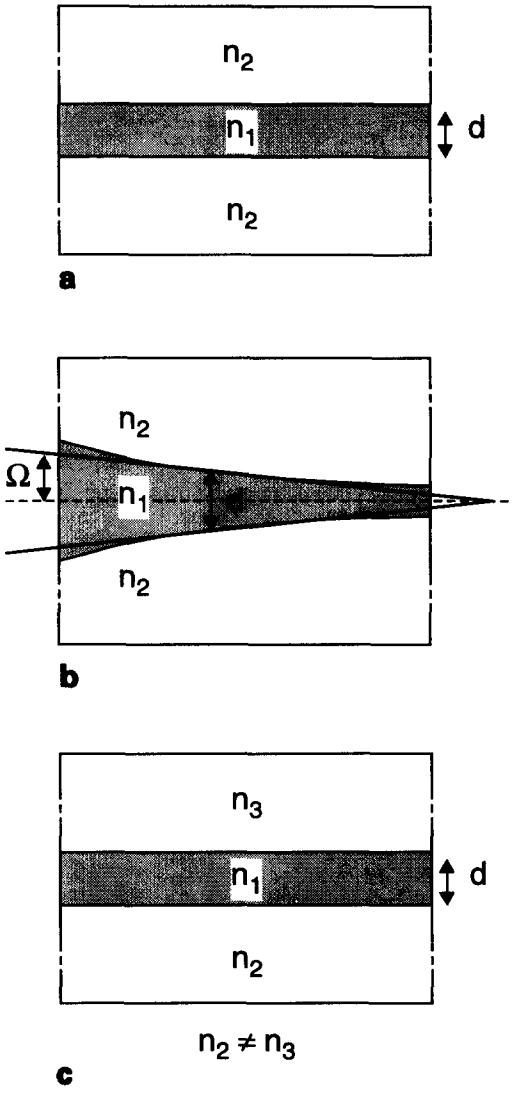

Fig. 2. (a) Symmetric slab waveguide; (b) tapered slab waveguide; (c) asymmetric slab waveguide.

local taper angle is limited by the following expression [7]:

$$\Omega < d\frac{(n_{eff} - n_2)}{2\lambda}$$

where Ω is half the local taper angle, d is the local thickness of the waveguide (see Fig. 1b),

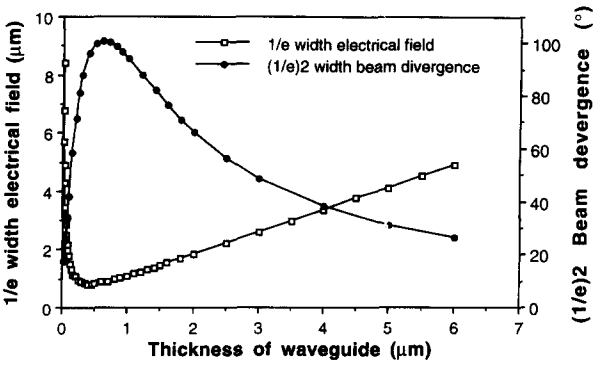

Fig. 3. 1/e width of the optical mode and $(1/e)^2$ width of the beam divergence in an InGaAsP/InP symmetric slab waveguide as a function of the thickness of the guiding layer.

n_{eff} ($n_2 < n_{eff} < n_1$) is the effective refractive index of the local mode and n_2 is the refractive index of the cladding layers. Indeed, we observe that for weakly guided modes (small n_{eff}, small d) in a down tapered waveguide, negligible power losses in the taper can only be obtained when the taper angle Ω is very small. For strongly guided modes, the maximal allowed taper angle Ω is much larger.

The simplest taper is a linear one. Since the maximal allowed taper angle in a down-taper is very small, the taper length that is necessary to obtain a large spotsize with negligible conversion loss will be very long in a linear taper. To reduce the taper length, more complicated taper profiles are recommended, such as parabolic, exponential or hyperbolic tapers [8]. With these profiles the thickness variation (and hence taper angle) decreases as the thickness of the guiding layer becomes smaller.

Furthermore, the minimal taper length is strongly dependent on the asymmetry of the waveguide structure (see Fig. 3c); the higher the asymmetry, the smaller the required taper angle and the longer the taper [9].

The lowest coupling losses (or field mismatch losses) are achieved when the semiconductor waveguide mode and the fibre mode are fully matched. The optical mode in a fibre has a quasi-Gaussian shape. Therefore, tapered waveguides are often designed to have a Gaussian mode-profile at the waveguide output facet. A large Gaussian field distribution can only be obtained with a very thick guiding layer which has a very small refractive index difference (order 10^{-3}) with respect to the cladding layers. As stated earlier, such a small refractive index difference can hardly be realized by compositional changes. A more realistic solution is based on the use of homostructure waveguides [10] or diluted structures [11–13]. The former structures consist of a non-intentionally doped layer (low n-type background concentration) deposited on a highly doped n-type substrate. In the latter structures, alternated layers of, for example, InGaAsP or InAlAs and InP produce the required equivalent index of the waveguide core. Generally, it is difficult to integrate these fibre-matched waveguide structures with other devices. Therefore, Kasaya has demonstrated that very low-loss butt-coupling is also achievable between the Gaussian-shaped fibre mode and the non-Gaussian (exponential-) shaped mode of a semiconductor waveguide with a very thin core [14]. He calculated that InGaAsP/InP waveguide structures can be connected to single-mode fibres with coupling losses below 0.5 dB.

3. Technological approaches to tapered devices

3.1 Taper designs

There are different ways in which to realize semiconductor mode size converters. Some tapered structures are presented in Fig. 4. For ease of drawing, all the tapers in this figure have a linear profile. The dark parts in the different tapered waveguide structures represent the guiding layers. There are vertical and lateral

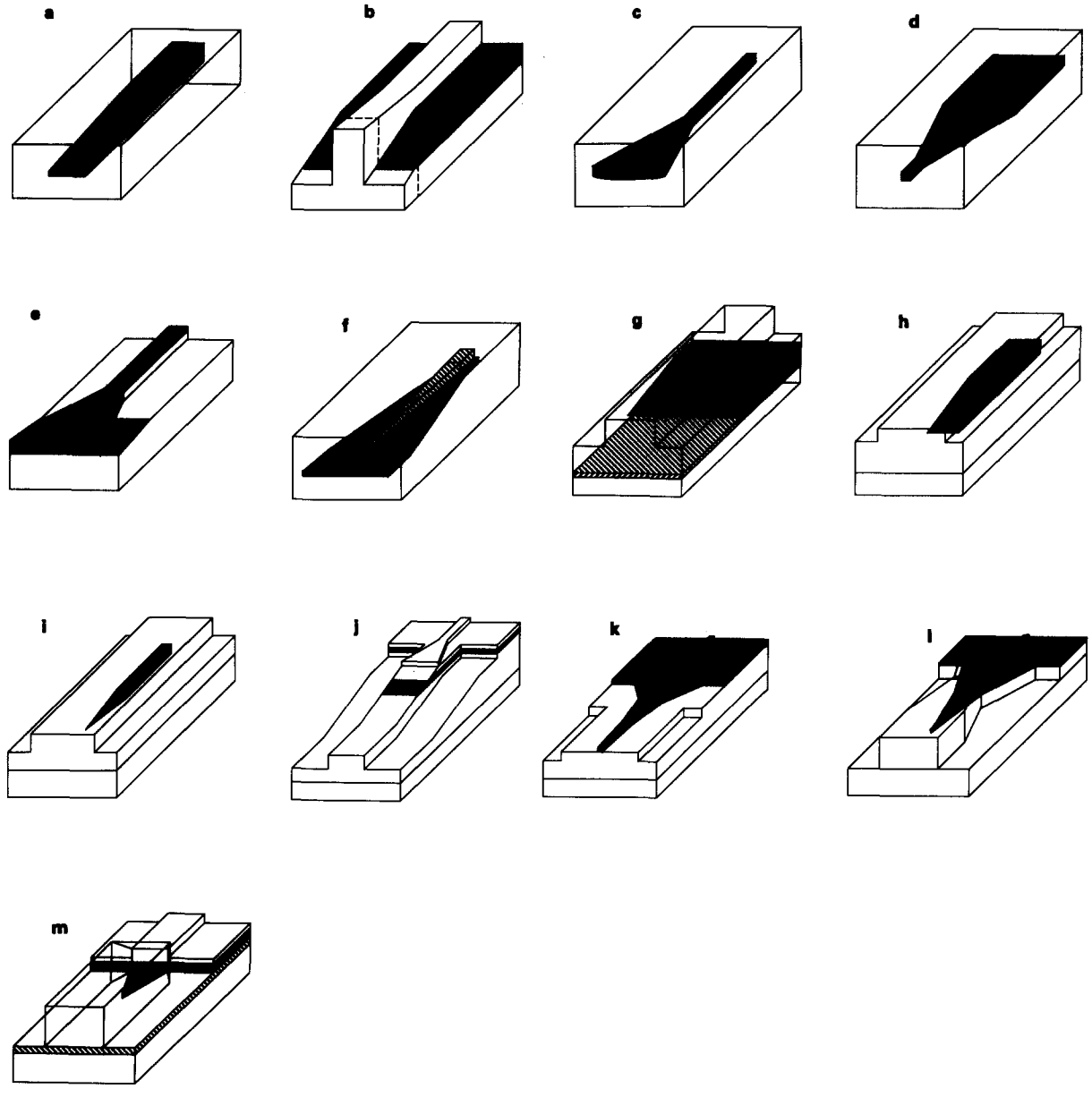

Fig. 4. Taper structures. (a) Vertical down-tapered buried waveguide; (b) vertical down-tapered ridge waveguide; (c) lateral up-tapered buried waveguide; (d) lateral down-tapered buried waveguide; (e) combined lateral and vertical ridge waveguide taper; (f) double lateral overlapping buried waveguide taper; (g) vertical overlapping ridge waveguide taper; (h) vertical overlapping waveguide taper transition from a buried waveguide to a fibre-matched waveguide; (i) two-dimensional overlapping waveguide taper transition from a buried waveguide to a fibre-matched waveguide; (j) overlapping waveguide taper transition with two sections from a ridge waveguide to a fibre-matched waveguide; (k) multisection overlapping taper transition from a ridge waveguide to a fibre-matched waveguide; (l) nested waveguide taper transition from a ridge waveguide to a fibre-matched waveguide; (m) nested overlapping ridge waveguide taper.

tapers or combinations of both. In a vertical taper the thickness of the guiding layer(s) is changed along the device. In a laterally tapered device, the width of the waveguide is changed. One can up-taper by increasing the waveguide dimensions near the end facet, or down-taper by decreasing the waveguide dimensions near the end facet.

Examples of one dimensional vertical tapers are given in Fig. 4a for a buried waveguide structure [15, 16] and in Fig. 4b for a ridge waveguide structure [17]. A facet needs to be cleaved at the position of the dashed line in Fig. 4b. Figures 4c and 4d show laterally up-tapered [18, 19] (resp. down-tapered [14, 20]) mode size converters. A combined lateral and vertical taper is shown in Fig. 4e [21].

A lot of mode size converters consist of overlapping waveguides, one or both of which can be tapered. The optical power is coupled from one waveguide to the other by means of a tapered transition region. It is important that the taper angle in the transition region is sufficiently small to prevent coupling of power from the fundamental mode into the higher order taper modes [22]. The waveguide near the end facet is often fibre matched. In Fig. 4f the small spotsize is transformed into the large spotsize by means of a double lateral taper [23]. Both waveguides have a buried structure. In Fig. 4g a strongly confined ridge waveguide is converted to a weakly confined ridge waveguide by means of a vertical taper [24]. Figs. 4h and 4i represent a one-dimensional (vertical) [10] (respectively two-dimensional [12]) tapered transition of a buried waveguide into a fibre matched waveguide. In Fig. 4j the transition from a ridge waveguide into a fibre matched waveguide is realized by a two section tapered transition region [25]. In the first section, the ridge is laterally tapered; in the second section, the top cladding and guiding layers are gradually removed. Finally, some more complex designs are shown in Figs. 4k [26], 4l [27] and 4m [28].

Although the overview of taper structures, as illustrated in Fig. 4, is not complete, it is clear that over the past few years much effort has been channelled into the design of III–V semiconductor mode size transformers.

3.2 Fabrication methods

We can see from Fig. 4 that some taper structures have a simple design while others have a quite complicated structure. There exist nearly as many fabrication methods as there are taper designs. The most straightforward technology to realize vertical tapers is the dip-etch process [24]. The waveguide taper is etched by dipping it in a controlled way into the etchant (see Fig. 5a). This etching technique is simple, but leads generally to fairly long tapered structures. Furthermore, it is impossible to process a full wafer.

A second wet etch technique is the dynamic etch mask technique [29]. The semiconductor is first covered with a thin-film material, which forms the dynamic mask and whose etch rate is significantly higher than the etch rate of the semiconductor material (Fig. 5b). This dynamic mask just covers the area where the taper is desired. The upper etch mask (e.g. photoresist or oxide) is subsequently deposited over the entire sample. This mask is opened near the dynamic mask at the place where the deeply etched end of the taper is desired. The taper is then chemically etched. Due to the high etch rate of the dynamic mask, more and more semiconductor material will be exposed to the etchant during etching. Taper structures with a length of only 50 μm have been realized in this way.

A third wet etch technique with which to realize vertical tapering is demonstrated by Brenner [17]. By partially covering the substrate with a SiO_x-mask and using a diffusion-limited wet etchant, the etch rate can be controlled laterally over the substrate (Fig. 5c). For narrower mask openings, enhanced etch rates are obtained.

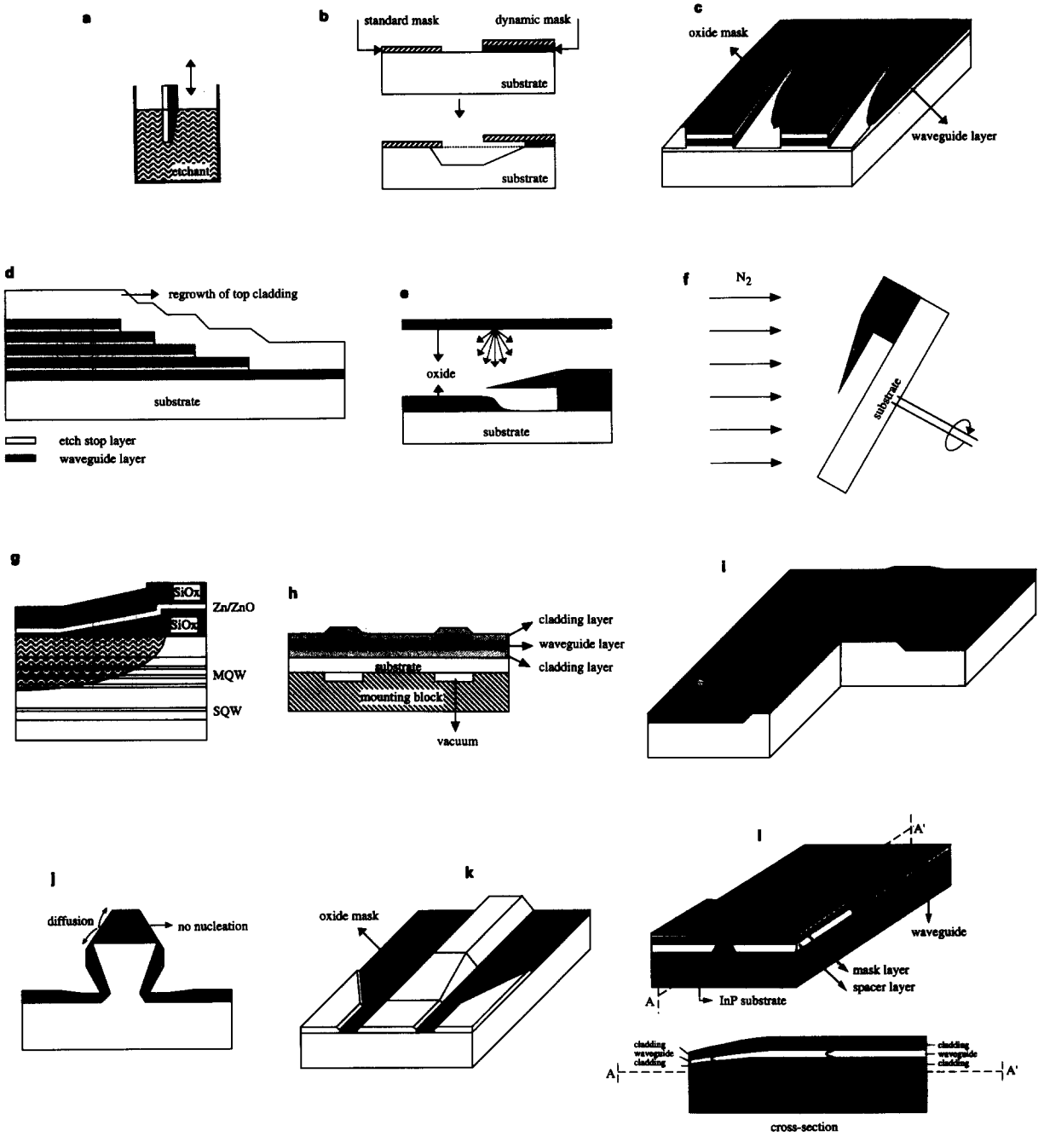

Fig. 5. Taper fabrication methods. (a) Dip-etch technique; (b) dynamic etch mask technique; (c) diffusion limited etch technique; (d) stepped etching; (e) oxide shadow technique; (f) direct shadow etching; (g) impurity-induced layer disordering (IILD); (h) temperature gradient during MBE; (i) LPE-growth on a ridge; (j) MOVPE-growth on a ridge; (k) selective area growth; (l) shadow masked growth.

The main disadvantages of the above wet etch techniques are low reproducibility and the difficulty of defining sophisticated taper profiles such as parabolic or exponential shapes.

A wet etch technique that allows more reproducible tapered profiles is the stepped reduction of the waveguide core thickness used by AT&T [30, 31]. Several etch-stop layers are embedded within the guiding layer to form a staircase profile by sequentially displaced masking and selective etching (Fig. 5d). A sufficient number of steps is required to allow adiabatic mode expansion. This technique is again quite simple but time consuming, since a lot of photolithographic and etching steps are needed.

The oxide shadow and direct shadow etching techniques, introduced by Siemens, allow the realization of vertical taper profiles using dry etch techniques [32] . For both techniques, a shadow mask made of silicon is fixed above the substrate on top of a spacer. For the oxide shadow technique, a tapered oxide layer is deposited on the substrate in a sputter chamber (Fig. 5e). This oxide profile is then transferred into the semiconductor by N_2 ion milling. The taper profile is controlled by the shape of the shadow mask. In case of direct shadow etching, the substrate with shadow mask is in a N_2 ion milling module with the axis of rotation tilted with respect to the direction of the ion beam (Fig. 5f). After etching, a tapered transition is observed in the semiconductor. The taper profile is now controlled by the tilt angle and the height of the spacer of the shadow mask. An evaluation by Müller has shown that both techniques are simple and reproducible, and allow a precise definition of the taper profile.

All the above described techniques require at least one regrowth step for the top cladding layer. The impurity-induced layer disordering (IILD) technique eliminates the need for regrowth in the fabrication process [33]. By Zn-diffusion through a tapered SiO_x barrier (Fig. 5g), the ions in a MQW are intermixed so that the quantum wells are gradually destroyed. As a result, the bandgap of the destroyed MQW increases, which means that the refractive index of the MQW-region decreases. This technique is suitable for interconnecting a MQW-waveguide to a single QW-waveguide. It appears to be difficult to optimize the diffusion profile.

There also exist techniques that allow *in situ* vertical tapering during epitaxial growth so that, unlike the previous techniques (except the impurity-induced layer disordering technique), the guiding layer and top cladding layer can be grown in a single growth step.

During molecular beam epitaxy (MBE) growth of AlGaAs, it is possible to obtain spatial variations in growth rate and composition by introducing a temperature gradient across the substrate, e.g. by using a mounting block whose top surface is slightly recessed in several regions (Fig. 5h) [34, 35]. Above 650°C the sticking coefficient of Ga decreases continuously with increasing temperature. Growing at temperatures above 650°C will therefore result in a spatial gradient in thickness and composition. When growing at lower temperatures, the sticking coefficient is insensitive to growth-temperature variations and the growth is uniform. Cladding layers are therefore grown at low temperatures, while the temperature is increased for the growth of the guiding layer. Both thickness and compositional variations result in a weaker confinement in the taper. The change in refractive index (due to the compositional change) accounts for 75% of the reduction in the vertical far-field beam divergence, while the change in vertical dimensions accounts for the remaining 25% of the reduction.

Due to the mass transport properties of liquid phase epitaxy (LPE)-growth [1] and the surface diffusion properties of metal organic vapour phase epitaxy (MOVPE)-growth [36], the growth rate on a ridge is dependent on the width

of the ridge. During LPE the growth rate decreases (Fig. 5i); during MOVPE the growth rate increases as the width of the ridge decreases (Fig. 5j).

Similar to the diffusion-limited etch technique, the growth rate in a MOVPE process will be enhanced when the substrate is covered by a SiO_x-mask (Fig. 5k) [17, 37]. This technique is better known as the 'selective area growth' technique. The larger the oxide stripe width, the smaller the mask opening, and the higher the growth pressure, the larger the growth rate enhancement [38]. The taper in Fig. 4b is realized by diffusion-limited etching of the guiding layer, followed by selective area growth of the cladding-layer using the same SiO_x-mask. In this way, the thickness of the cladding layer will increase as the optical mode size increases.

The last *in situ* technique we describe is the shadow masked growth (SMG) technique, which has been developed at our laboratory [39, 40]. SMG uses a monocrystalline mask held by means of a spacer layer at a certain distance above the substrate (Fig. 5l). During epitaxial growth, the deposition on the substrate takes place through the window in the shadow mask. Thickness changes are fully controlled by the lateral dimensions of the shadow mask and the reactor pressure: the smaller the mask window and the higher the reactor pressure, the larger the growth rate reduction relative to the nominal growth rate on a non-masked substrate.

The SMG and selective area growth techniques are very similar. During SMG the growth rate decreases, while during selective area growth the rate increases. Both techniques show not only thickness variations but also compositional variations [40, 41]. In both cases, tapering is the result of the co-operation between thickness reduction and compositional changes. In most tapered devices the thickness of the waveguide layer is decreased near the end of the taper. For this reason, the SMG-technique is advantageous to the selective area growth technique. The nominal (uniform) waveguide layer can be grown on the non-masked part of the substrate during SMG, enabling high quality layers. On the contrary, the nominal waveguide layer must be grown selectively when using the area selective growth technique. A drawback of the SMG technique is the additional growth step of the shadow mask and an additional processing step needed to remove the shadow mask. However, this drawback might be eliminated by using a mechanical mask instead of a monocrystalline mask [42, 43]. This mechanical mask is then placed on top of the substrate and can be removed easily afterwards.

Laterally tapered waveguides can be achieved by standard lithography and wet chemical etching, or by a combination of electron beam (e-beam) writing and reactive ion etching (RIE). The first method is very simple, but does not allow the etching of very fine structures. The second method offers a high spatial resolution, but is expensive.

4. Tapered waveguiding devices

4.1 Tapered waveguides

In Table 1 an overview is given of tapered waveguides realized by different research groups. First the type of taper is given: lateral (L), vertical (V) or a combination of both (V + L). The third column shows the fabrication technique applied. The fourth column contains the wavelength of the guided light. Then some measurement results are summarized, such as the lateral (L) and vertical (V) dimensions of the spotsize, the lateral (L) and vertical (V) alignment tolerances, the coupling loss (field mismatch loss) when the light of the waveguide is coupled into a single mode cleaved or lensed fibre (F), and the taper loss. An arrow in the columns of the spotsize dimensions indicates an increase of the spotsize along the taper. If only one value is given, this is the dimension of the largest spot size. Some

TABLE 1 Overview of tapered waveguides

Group	Taper	Technique	λ (nm)	Spotsize		Align. tol. (±)		Coupl. loss (dB)	Taper *loss* (dB)	Remarks	Ref.
				L (μm)	V (μm)	L (μm)	V (μm)				
Siemens	V	Ox. shad. etch	1550	2.0 → 7.7 (FWHM)	1.5 → 4.7 (FWHM)	3 (1 dB)	2.1 (1 dB)	<2 (cleaved F)		AR coating	[44, 10] Figs. 4h & 5e
Siemens	V + L	Dir. shad. etch (V) + stand. litho (L)	1550			4 (3 dB)	3 (3 dB)	1.5 (cleaved F)			[25, 45] Figs. 4j & 5f
Siemens	L	RIE	1550	4.5 → 12 ($1/e^2$)	2.5 → 5.5 ($1/e^2$)	4 (1 dB)	2 (1 dB)		0.7		[27] Fig. 4k
ETHZ	V	Dip-etch	1530			0.8 (1 dB)	0.8 (1 dB)	1.7 (lensed F) 8.3 (cleaved F, 10 μm spotsize)	< 0.5	AR coating	[24] Figs. 4g & 5a
ETHZ	V	Diff. lim. etch + Sel. growth	1530	4 ($1/e^2$)	0.7 → 2.7 ($1/e^2$)			0.9 (lensed F)		AR coating	[17] Figs. 4b & 5d + k
DBP Telekom	L	e-beam + RIE	1550	1.4 → 8	1 → 8			0.6 (cleaved F, 7.7 μm spotsize)	0.1	Non-linear taper Index matching liquid	[46] Fig. 4f
DBP Telekom	L	e-beam + RIE	1550	2.3 → 8.2 ($1/e^2$)	2 → 5.1 ($1/e^2$)			1 (cleaved F, 8 μm spotsize)		Linear taper Index matching liquid	[23] Fig. 4f
ANT	L	e-beam + RIE	1300–1500	3 → 12 (FWHM)	2.2 → 5 (FWHM)			4 (cleaved F, 10 μm spotsize)			[28] Fig. 4l
NTT	L	RIBE, Wet etch + Sel. growth	1550					2.3 (cleaved F, 4 μm spotsize)*		AR coating *including taper loss	[29] Figs. 4m & 5k
NTT	L	e-beam + RIE	1550	1.5 → 3	(< 1) → 3	2.5 (1 dB)	2.5 (1 dB)	0.9 (cleaved F, 4.5 μm spotsize)	0.3		[47] Fig. 4d
NTT	V + L	Step. etch (V) + RIE (L)	1550	2.4 → 6.5 ($1/e^2$)	2.2 → 4.5 ($1/e^2$)	2.7 (1 dB)		0.4 (cleaved F)			[12] Figs. 4i & 5c
Bellcore	V + L	Sel. growth (V) + RIE (L)	1540	2.9 → 6.2 ($1/e^2$)	1.6 → 4.5 ($1/e^2$)			2.6 (cleaved F, 10 μm spotsize)	0.35	AR coating	[21] Figs. 4e & 5k
Bellcore	V	Dyn. etch mask	1520		2 → 4 (FWHM)				< 0.2		[29] Fig. 5b
Univ. of Florida	V	IILD	895	1 → 1.6 ($1/e^2$)							[33] Fig 5g
MIT Lincoln Lab.	V	ΔT (MBE)	880	0.71 → 0.97 ($15.7^2 \rightarrow 10^2$) (FWHM)						Antenna with high directional farfield	[34, 35] Fig. 5h
Our work	V	Shad. mask. growth	1550	5.0 → 3.4	1.6 → 2.2	1.2 (1 dB)	1.2 (1 dB)	1.7 (lensed F)*		*including taper loss	[48] Fig. 5l

groups measure the FWHM (Full Width at Half Maximum) values of the spotsize, others measure $1/e^2$-values. Some groups do not mention which value of the spotsize has been measured. The value between brackets in the columns for the alignment tolerance measurements gives the coupling loss increase corresponding to the lateral or vertical displacement. One should be careful when comparing coupling losses to cleaved fibres, since fibres with different spotsizes (ranging from 4–10 μm) are used by different research groups. The last two columns contain some remarks and references. In the last column, we also refer to the corresponding taper design and fabrication technique in Figs. 4 and 5.

From Table 1, it is clear that most effort is expended in the fabrication of tapered waveguides for light at 1.55 μm. By integrating a taper with a semiconductor waveguide, most researchers want to reduce the insertion losses and the packaging costs of opto-electronic integrated circuits (OEICs) in future optical communication networks. The University of Florida wanted to improve the integration and interconnection of opto-electronic devices with different mode sizes on a single chip. Therefore, they developed the IILD technique to couple light from a MQW waveguide into a single quantum well waveguide. MIT developed a reduced confinement AlGaAs tapered waveguide antenna with an enhanced far field beam directionality for use in coupling to free space radiation.

In tapers with a fibre matched waveguide at the end, large spot sizes and hence large alignment tolerances and low coupling losses can be obtained. The lowest coupling loss to cleaved fibres is only 0.4 dB, which means that 91% of the light can be coupled into the fibre. In this case the (1 dB) alignment tolerances are larger than 2 μm. This should be compared to untapered small spot size waveguides which have coupling losses of typically 10 dB (only 10% of the light can be coupled into the fibre) and alignment tolerances below ± 1 μm. When the taper structure is well designed, taper losses can be kept very small (below 0.5 dB). The lowest taper loss, only 0.1 dB, is achieved by DBP Telekom by using a non-linear lateral taper.

Our vertically tapered waveguides are realized with the pressure engineered shadow masked growth technique. The waveguide layer is grown at atmospheric pressure to obtain the largest possible growth rate reduction (factor 3). The cladding layers are grown at low pressure to limit the growth rate reduction (factor 2). After lift-off of the shadow mask, a ridge was etched. The height of this ridge is not optimal in the tapered region. Since the thickness of the top cladding layer in the tapered region is smaller than in the non-tapered region, the lateral confinement in the taper becomes stronger near the end of the taper, even if an etch stop layer is provided. This explains why the lateral dimension of the spotsize in the tapered waveguide becomes smaller (Table 1). Normally one prefers to reduce the lateral confinement in a waveguide taper. In our case, due to the enhanced lateral confinement, we obtained a quasi circular spotsize, which enabled a low coupling loss (1.7 dB) to a lensed fibre. However, an enhanced lateral confinement in the taper can cause a vertically asymmetric mode, and this might result in high taper losses. For the longest shadow masked grown tapered waveguides (with a large thickness reduction at the end), we have indeed measured high taper losses (> 3 dB).

4.2 Tapered laser diodes

A similar overview as in the previous section is given in Table 2 for tapered lasers. Most columns in Table 2 give the same information as in Table 1, but instead of the spotsize, the FWHM values of the beam divergence are given now. The taper losses are not given here, since it is not straightforward to measure the taper loss in a laser device. Column 5 describes the type of laser. The different laser structures are BTRS

TABLE 2 Overview of tapered laser diodes

Group	Taper	Technique	λ (nm)	Laser type	I_{thr} (mA)	QE (%)	Beam divergence (FWHM)		Align. tol. (±)		Coupl. loss (dB)	Ref.
							L (°)	V (°)	L (μm)	V (μm)		
Mitsubishi	V	LPE-growth on ridge	780	BTRS, DH	50 → 60 (CW)	42 (coatings)	9	10				[1] Fig. 5i
AAR	L	e-beam + RIE	1.48	BRS, Str.MQW	15 → 25 (CW)	58 → 52 (coatings)	19 → 13	22 → 15	1.3 (0.5 dB)	1.3 (0.5 dB)	1.4 (lensed F) 5.2 (cleaved F)	[50] Fig. 4d
Fujitsu	V	Sel. growth	1.3	PBH, MQW	19 (CW)	21 (no coatings)	25 → 8	35.4 → 11.8	2 (1 dB)	2 (1 dB)	3.1 (cleaved F)	[15] Figs. 4a & 5k
MIT Lincoln Lab.	L	Wet etch + Cylindrical facet	1.3	PBH, DH	25		40 → 9.2					[19] Fig. 4c
NIT	L	e-beam + RIE	1.55	PBH, DBR, DH	9 (CW)	21	12	12	2 (1 dB)	2 (1 dB)	2.8 (cleaved F, 4 μm spotsize)	[47] Fig. 4d
AT&T	V + L	Step. etch (V) Wet etch (L)	1.5	PBH, DBR, Str. MQW	52 (CW)	30 (coatings)	12	12	3.8 (1 dB)	2.1 (1 dB)	4.2 (cleaved F, 8 μm core)	[30] Fig. 5c
AT&T	V	Step. etch	1.5	PBH, MQW	28 (CW)	17	10	15	3 (1 dB)	2 (1 dB)	5 (cleaved F)	[31] Fig. 5c
BTL	L		1.56	PBH, MQW	8.5 → 11.5 (CW)		40 → 16	39 → 15			4.6 (cleaved F, 10 μm core)	[7] Fig. 4f
BTL	L		1.6	PBH, Str. MQW	4.2 → 4.9 (CW)	31	27 → 11	27 → 11			4.1 (cleaved F, 10 μm core)	[50] Fig. 4f
Our work	V	Shad. mask. growth	1.55	PBH, DH	16 → 34 (CW)	18 (no coatings)	32 → 13	42 → 15	1 (1 dB) 2.1 (1 dB)	1 (1 dB) 1.9 (1 dB)	1.6 (lensed F) 4.8 (cleaved F, 8 μm core)	[16, 48] Figs. 4a & 5l
Our work	V	Shad. mask. growth	1.5	PBH, Str. MQW	7 → 8.2 (CW)	28.2 → 31.5 (no coatings)	32 → 11.8	33.6 → 16.6	2.3 (1 dB)	2.4 (1 dB)	2.8 (cleaved F, 8 μm core)	To be published Figs. 4a & 5l
Our work	V	Shad. mask. growth	980	Ridge, Str. QW	8.3 → 11.2 (CW)	33 → 36 (no coatings)	15	47 → 29(21)				[51] Fig. 5l

(buried twin-ridge substrate), BRS (buried ridge stripe), PBH (planar buried heterostructure) and Ridge. The possible active regions are DH (double heterostructure), (M)QW ((multi) quantum well) and Str. MQW (strained multi quantum well). Most laser devices are Fabry-Perot lasers. Two lasers are DBR (Distributed Bragg Reflector) lasers. Columns 6 and 7 give the threshold current and the differential quantum efficiency of the laser diodes. If only one value is shown, then these are the values for the tapered laser device. An arrow indicates the change in threshold current or quantum efficiency due to the tapering. In a good tapered laser device, the threshold current and quantum efficiency should not increase (resp. decrease) much compared to non-tapered reference lasers. This means that for the same injection current more power can be coupled from the tapered laser diode.

The Mitsubishi AlGaAs laser, emitting at 780 nm, is used as a light source in an optical disk system. The narrow beam of the tapered laser enables a high coupling efficiency with the optical components, and therefore the high power (6–8 mW), necessary for writing signals on the disk surface, can be easily obtained. Besides, the reduced confinement in the tapered active layer increases the COD power level and the operating lifetime.

The other lasers in Table 2 are used in optical communication networks. The 1.48 μm and the 980 nm lasers are pump lasers for fibre amplifiers. The 1.3 and ($\pm$) 1.5 μm lasers are light sources for optical networks. In all those lasers the beam divergence is decreased by integrating a taper so that more light can be coupled into the optical fibre. The lowest coupling loss (to a cleaved fibre) ever obtained is 2.8 dB for the laterally tapered DBR laser, realized by NTT. The lateral dimension of the tapered waveguide region is decreased from 1.2 μm to 0.45 μm, resulting in a beam divergence of only 12° for both directions.

Other laterally tapered laser devices were realized by MIT, AAR and BTL. The cylindrical mirror facet in the MIT laser is fabricated by selective chemical etching followed by a mass transport technique, which smoothes the etched surface to obtain high optical quality. The cylindrical facet provides a good reflective feedback and simultaneously forms an output lens which reduces the beam divergence. In this way, the lateral divergence was reduced from 40° to 9.2°.

The BRS laser of AAR is laterally tapered from 2 μm to 0.7 μm. The tapered region is divided into three linear sections with decreasing slopes, which is more adiabatic than a linear taper. The lateral (resp. vertical) divergence is improved by 6° (resp. 7°).

The design of the BTL tapered laser is very similar to that presented in Fig. 3f: only the top waveguide (active region) is laterally tapered – the underlying passive guide now has a constant width. In the case of a strained multi quantum well active region, a circular beam with a divergence of only 11° was obtained. The BTL tapered lasers show the lowest threshold currents. The threshold current increase due to the tapering is very small (only 0.7 mA for a strained MQW laser).

A lot of tapered lasers consist of a vertical taper. Since the MQW active region of the Fujitsu laser is selectively grown, its thickness is 4.7 times larger than the thickness in the taper, which is grown in a non-masked area on the substrate. As a result, both beam divergences are reduced by a factor 3 to a beam of 8° × 11.8°.

Using the shadow masked growth technique, we are able to reduce the active layer thickness in the taper by a factor 3 for the 1.55 μm DH laser, and so we could obtain a beam divergence of 13° × 15° starting from a beam divergence of 32° × 42° for a non-tapered laser. Similar results are obtained for 1.5 μm strained MQW lasers. Recent measurements reveal coupling losses as

low as 2.8 dB. The ridge structure, however, is not as convenient to realize tapered devices as the buried structure, because of the enhanced lateral confinement (see the previous discussion on the SMG tapered waveguides). Like the tapered waveguides, the 980 nm InGaAs/AlGaAs ridge laser is grown, making use of the pressure engineered SMG technique. The vertical divergence was decreased from 47° to 29°. We note that narrower vertical divergences could be achieved, but only at a higher threshold current and a reduced quantum efficiency.

AT&T has realized 1.5 μm tapered lasers using the stepped etch technique. A first tapered laser was a Fabry-Perot laser which had a beam divergence of $10° \times 15°$. The second tapered laser is a DBR laser. Next to the stepped etching, the mesa width is gradually increased from 2.5 to 5 μm to expand the mode in the lateral direction. Now a circular beam with a divergence of 12° is obtained.

5. Conclusion

During the past few years (especially the last three years), much attention has been paid to the monolithic integration of spot size transformers with III–V semiconductor devices, in order to reduce the insertion loss and packaging costs in future optical communication networks. A careful design of the taper structure is necessary to match the waveguide mode size to that of a single mode fibre with a minimal mode conversion loss.

A lot of taper designs have been proposed, and nearly as many fabrication technologies developed. Some of those technologies are simple and make use of low-cost equipment, but do not offer a high resolution or a high reproducibility. Other fabrication techniques, which are much more reproducible and allow high resolution taper profiles, are often more complex and time consuming, or require expensive installations. In future, when tapered devices go into large scale production, the most simple technologies offering a reasonable yield might survive.

Research activity on tapered devices is still increasing, as is the performance of such devices. Currently, tapered waveguides can be fabricated with a coupling loss of 0.4 dB and a taper loss of only 0.1 dB. The best tapered lasers show coupling losses around 3 dB and beam divergences of $12° \times 12°$.

Acknowledgements

I. Moerman, G. Vermeire, J. Blondelle and W. Vanderbauwhede thank the IWT (Flemish institute for the promotion of scientific-technological research in the industry) for financial support. J. Haes is acknowledged for helpful discussions. Part of this work is supported by the European projects UFOS (RACE) and MOSAIC (ESPRIT).

References

[1] T. Murakami *et al.*, A very narrow-beam AlGaAs laser with a thin tapered thickness active layer (T^3-laser), *IEEE J. Quantum Electronics*, QE-23(6) (1987) 712–719.

[2] J. Haes, J. Willems and R. Baets, Design of adiabatic tapers for high contrast step index waveguides, *International Symposium on Integrated Optics, Lindau, 1994*, Paper 2212-74.

[3] J.D. Love, W.M. Henri, W.J. Stewart, R.J. Black, S. Lacroix and F. Gonthier, Tapered single-mode fibres and devices, Part 1: Adiabaticity criteria, *IEE Proc. J.*, 138(5) (1991) 343–354.

[4] R.J. Black, S. Lacroix, F. Gonthier and J.D. Love, Tapered single-mode fibres and devices, Part 2: Experimental and theoretical quantification, *IEE Proc. J.*, 138(5) (1991) 355–364.

[5] K.-H. Schlereth and M. Tacke, The complex constant of multilayer waveguides: an algorithm for a personal computer, *IEEE J. Quantum Electronics*, 26(4) (1990) 627–630.

[6] J.K. Butler and J. Zoroofchi, Radiation fields of GaAs(Al)GaAs Injection lasers, *IEEE J. Quantum Electronics*, QE-10(10) (1974) 809–815.

[7] I.F. Lealman, L.J. Rivers, M.J. Harlow, S.D. Perrin

and M.J. Robertson, 1.56 μm InGaAsP/InP tapered active layer multiquantum well laser with improved coupling to cleaved single mode fibre, *Electr. Lett.*, 30(11) (1994) 857–859.

[8] G.R. Hadley, Design of tapered waveguides for improved output coupling, *IEEE Photonics Technology Lett.*, 5(9) (1993) 1068–1070.

[9] P.G. Suchoski, Jr. and R.V. Ramaswamy, Design of single-mode step-tapered waveguide sections, *IEEE J. Quantum Electr.*, QE-23(2) (1987) 205–211.

[10] G. Müller, B. Stegmüller, H. Westermeier and G. Wenger, Tapered InP/InGaAsP waveguide structure for efficient fibre-chip coupling, *Electr. Lett.*, 27(20) (1991) 1836–1838.

[11] C. Caldera, S. Morasca, G. Schiavini and A. Stano, Coupling between fibres and semiconductor waveguides: modelling and experiments with conventional and advanced structures, *Proceedings COST240 Workshop, Zürich, Switzerland, November 1991*, pp. 29–31.

[12] N. Yoshimoto, K. Kawano, H. Takeuchi, S. Kondo and Y. Noguchi, Spot size convertors using InP/InAlAs multi quantum well waveguides for low-loss singlemode fibre coupling, *Electr. Lett.*, 28(17) (1992) 1610–1611.

[13] R.J. Deri, N. Yasuoka, M. Makiuchi, A. Kuramata and O. Wada, Efficient fiber coupling to low-loss diluted multiple quantum well optical waveguides, *Appl. Physics Lett.*, 55(15) (1989) 1495–1497.

[14] K. Kasaya, O. Mitomi, M. Naganuma, Y. Kondo and Y. Nogushi, A simple laterally tapered waveguide for low loss coupling to single-mode fibers, *IEEE Photonics Technology Lett.*, 5 (3) (1993) 345–347.

[15] H. Soda, H. Kobayashi, M. Ekawa, N. Okazaki, O. Aoki, S. Ogita, T. Watanabe and S. Yamazaki, Tapered thickness spot-size transformer integrated BH MQW lasers, *Proceedings Integrated Photonic Research Conference*, San Francisco, CA, USA, February 1994.

[16] I. Moerman *et al.*, Monolithic integration of a spot size transformer with a planar buried heterostructure InGaAsP/InP-laser using the shadow masked growth technique, *IEEE Photonics Technology Lett.*, 51(8) (1994).

[17] T. Brenner and H. Melchior, Integrated Optical Modeshape Adapters in InGaAsP/InP for efficient fiber-to-waveguide coupling, *IEEE Photonics Technology Lett.*, 50(9) (1993) 1053–1056.

[18] G. Bendelli, K. Komori and S. Arai, Gain saturation and propagation characteristics of index-guided tapered waveguide traveling-wave semiconductor laser amplifiers (TTW-SLAs), *IEEE J.Quantum Electr.*, 28(2) (1992) 447–457.

[19] J.N. Walpole, Z.L. Liau, L.J. Missaggia and D. Yap, Diode lasers with cylindrical mirror facets and reduced beam divergence, *Appl. Physics Lett.*, 50(18) (1987) 1219–1221.

[20] P. Doussiere, P. Garabedian, C. Graver, E. Derouin, E. Gaumont-Gaorin, G. Michaud and R. Meilleur, Tapered active stripe for 1.5 μm InGaAsP/InP strained multiple quantum well lasers with reduced beam divergence, *Appl. Physics Lett.*, 64(5) (1994) 539–541.

[21] R.J. Deri, C. Caneau, E. Colas, L.M. Schiavone, N.C. Andreadakis, G.H. Song and E.C.M. Pennings, Integrated optic mode-size tapers by selective organometallic chemical vapor deposition of InGaAsP/InP, *Appl. Physics Lett.*, 61(8) (1992) 952–954.

[22] S. Misawa, M. Aoki, S. Fujita and K. Yokomori, Estimation of light wave transfer between three and four layered slab waveguides by tapered transition, *Technical Digest of the Fourth Microoptics Conference and the Eleventh Topical Meeting on Gradient-Index Optical Systems*, Kawasaki, Japan, October 1993, pp. 122–125.

[23] R. Zengerle, H. Brückner, H. Olzhausen and A. Kohl, Low-loss fibre-chip coupling by buried laterally tapered InP/InGaAsP waveguide structure, *Electr. Lett.*, 28(7) (1992) 631–632.

[24] T. Brenner, W. Hunziker, M. Smit, M. Bachmann, G. Guekos and H. Melchior, Vertical InP/InGaAsP tapers for low-loss optical fibre-waveguide coupling, *Electr. Lett.*, 28(22) (1992) 2040–2041.

[25] G. Müller, L. Stoll, G. Wenger and M. Schienle, First low loss InP/InGaAsP optical switch with integrated mode transformers, *Proceedings 19th European Conference on Optical Communication ECOC '93*, Montreux, Switzerland, 1993, pp. 37–40.

[26] J.G. Bauer, M. Schier and G. Ebbinghaus, High responsivity Integrated Tapered waveguide PIN Photodiode, *Proceedings 19th European Conference on Optical Communication ECOC '93*, Montreux, Switzerland, 1993, pp. 277–280.

[27] Th. Schwander, S. Fischer, A. Krämer, M. Laich, K. Luksic, G. Spatschek and M. Warth, Simple and low-loss fibre-to-chip coupling by integrated field-matching waveguide in InP, *Electr. Lett.*, 29(4) (1993) 326–328.

[28] K. Kawano, M. Kohtoku, N. Yoshimoto, S. Sekine and Y. Noguchi, 2 × 2 InGaAlAs/InAlAs multiquantum well (MQW) directional coupler waveguide switch modules integrated with spotsize convertors, *Electr. Lett.*, 30(4) (1994) 353–355.

[29] A. Shahar, W.J. Thomlinson, A. Yi-Yan, M. Seto and R.J. Deri, Dynamic etch mask technique for fabricating tapered semiconductor optical waveguides and other structures, *Appl. Physics Lett.*, 56(12) (1990) 1098–1100.

[30] T.L. Koch, U. Koren, G. Eisenstein, M.G. Young, M. Oron, C.R. Giles and B.I. Miller, Tapered wave-

guide inGaAs/InGaAsP multiple-quantum-well lasers, *IEEE Photonic Technology Lett.*, 2(2) (1990) 88–90.
[31] M. Chien, Ú. Koren, T.L. Koch, B.I. Miller, M. Oron, M.G. Young and J.L. Demiguel, Short cavity distributed bragg reflector laser with an integrated tapered output waveguide, *IEEE Photonics Technology Lett.*, 3(5) (1991) 418–420.
[32] G. Müller, G. Wender, L. Stoll, H. Westermeier and D. Seeberger, Fabrication techniques for vertically tapered InP/InGaAsP spot-size transformers with very low loss, *Proceedings European Conference on Integrated Optics ECIO 93*, Neuchâtel, Switzerland, pp. 14–15.
[33] H.S. Kim, S. Sinha and R.V. Ramaswamy, An MQW-SQW tapered waveguide transition, *IEEE Photonic Technology Lett.*, 5(9) (1993) 1049–1052.
[34] D.E. Bossi, W.D. Goodhue, M.C. Finn, K. Rauschenbach, J.W. Bales and R.H. Rediker, Reduced-confinement antennas for GaAlAs integrated optical waveguides, *Appl. Physics Lett.*, 56(5) (1990) 420–422.
[35] D.E. Bossi, W.D. Goodhue, L.M. Johnson and R.H. Rediker, Reduced-confinement GaAlAs tapered waveguide antennas for enhanced far-field beam directionality, *IEEE J. Quantum Electr.*, 27(3) (1991) 687–695.
[36] E. Colas, A. Shahar and W.J. Tomlinson, Diffusion-enhanced epitaxial growth of thickness-modulated low-loss rib waveguides on patterned GaAs substrates, *Appl. Physics Lett.*, 56(10) (1990) 955–957.
[37] E. Colas, C. Caneau, M. Frei, E.M. Clausen, Jr., W.E. Quinn and M.S. Kim, In situ definition of semiconductor structures by selective area growth and etching, *Appl. Physics Lett.*, 59(16) (1991) 2019–2021.
[38] G. Coudenys, G. Vermeire, Y. Zhu, I. Moerman, L. Buydens, P. Van Daele and P. Demeester, Novel growth techniques for the fabrication of photonic integrated circuits, *Materials Research Society Symposium Proceedings*, Vol 240, 1992, pp. 15–26.
[39] P. Demeester, L. Buydens and P. Van Daele, Growth velocity variations during metalorganic vapor phase epitaxy through an epitaxial shadow mask, *Appl. Physics Lett.*, 57(2) (1990) 168–170.
[40] G. Coudenys, I. Moerman, Z.Q. Yu, F. Vermaerke, P. Van Daele and P. Demeester, Atmospheric pressure and low pressure shadow masked MOVPE growth of InGaAs(P)/InP and (In)GaAs/(Al)GaAs heterostructures and quantum wells, *J. Electr. Materials*, 23(2) (1994) 227–234.
[41] T. Sasaki, M. Kitamura and I. Mito, Selective metal-organic vapor phase epitaxial growth of InGaAsP/InP layers with bandgap energy control in InGaAs/InGaAsP multiple-quantum well structures, *J. Crystal Growth*, 132 (1993) 435–443.
[42] J. Blondelle, I. Moerman, P. De Dobbelaere, P. Van Daele and P. Demeester, Advanced structures for integrated optics realized with shadow masked growth, *IEEE/LEOS Summer Topical Meeting on Optoelectronic Materials Growth and Processing*, Lake Tahoe, July 1994.
[43] S.M. Bedair, M.A. Tischler and T. Katsuyama, *Appl. Physics Lett.*, 48 (1986) 30.
[44] G. Wenger, G. Müller, B. Sauer, D. Seeberger and M. Honsberg, Highly efficient multi-fiber-chip coupling with large alignment tolerances by integrated InGaAsP/InP spot-size transformers, *Proceedings 18th European Conference on Optical Communication ECOC '92*, Berlin, Germany, 1992, pp. 927–930.
[45] Private communication.
[46] R. Zengerle, H.J. Brückner, E. Kuphal and O. Leminger, Low-loss fibre-chip-fibre butt coupling by buried nonlinearly tapered InP/InGaAsP waveguides, *Proceedings 19th European Conference on Optical Communication ECOC '93*, Montreux, Switzerland, 1993, pp. 249–252.
[47] K. Kasaya, Y. Kondo, M. Okamoto, O. Mitomi and M. Naganuma, Monolithically integrated DBR lasers with simple tapered waveguide for low-loss fibre coupling, *Electr. Lett.*, 29(23) (1993) 2067–2068.
[48] I. Moerman *et al.*, Vertically tapered InGaAsP/InP waveguides and lasers resulting in low-loss fibre-chip coupling, *Proceedings 20th European Conference on Optical Communication ECOC '94*, Firenze, Italy, 1994.
[49] P. Doussiere, P. Garabedian, C. Graver, E. Derouin, E. Gaumont-Goarin, G. Michaud and R. Meilleur, Taper active stripe for 1.5 μm InGaAsP/InP strained multiple quantum well lasers with reduced beam deivergence, *Appl. Physics Lett.*, 64(5) (1994) 539–541.
[50] I.F. Lealman, C.P. Seltzer, L.J. Rivers, M.J. Harlow and S.D. Perrin, Low threshold current 1.6 μm InGaAsP/InP tapered active layer multiple quantum well laser with improved coupling to cleaved single mode fibre, *Electron. Lett.*, 30(12) (1994) 973–975.
[51] G. Vermeire, F. Vermaerke, I. Moerman, J. Haes, R. Baets, P. Van Daele and P. Demeester, Monolithic integration of a SQW laser diode and a mode-size convertor using shadow masked MOVPE growth, *J. Crystal Growth*.